Effect of plasma shaping and resonance location on minority ion temperature anisotropy in tokamak plasmas heated with ICRH

Ye O Kazakov[1], T Fülöp[1], I Pusztai[1] and T Johnson[2]

[1] Department of Applied Physics, Chalmers University of Technology, Euratom-VR Association, SE-41296 Göteborg, Sweden
[2] School of Electrical Engineering, Royal Institute of Technology, Euratom-VR Association, Stockholm, Sweden

E-mail: kazakov@chalmers.se

Abstract. Poloidal asymmetries of the impurity distribution, which are observed in tokamaks, may influence the impurity cross-field transport. Low field side ion cyclotron resonance heating (ICRH) often results in an inboard accumulation of impurities, which may in turn lead to an outward convective impurity flux. The temperature anisotropy of the ICRH-heated minority ions is identified to be one of the main parameters governing the impurity asymmetry strength. In the present work we analyze the effect of plasma shaping and the ICRH resonance location on the minority temperature anisotropy by means of the TORIC-SSFPQL modelling. We find that ellipticity reduces the anisotropy level due to the wave defocussing and broader absorption regions for the elongated plasmas. The temperature anisotropy decrease in case of the resonance layers located closer to the edge is caused by the significant reduction in heating power densities due to geometrical reasons.

1. Introduction

Ion cyclotron resonance heating (ICRH) is a widely used heating method in present-day fusion devices and is foreseen to be installed in ITER. In connection with ICRH the impurity density becomes often poloidally asymmetric [1–3]. The main reason for the asymmetry is an increase in the minority density at the outboard side of the magnetic surface due to ICRH. Preferentially perpendicular heating of the minority ions by ICRH traps excessive amount of positive charges at the smaller B locations and thus generates poloidal electrostatic electric field [4] that pushes impurities to the opposite (inboard) side. In recent experiments at the Alcator C-Mod tokamak it was conclusively demonstrated the link of the asymmetry level to ICRH [3]. In contrast to NBI-heated plasmas, where centrifugal effects usually lead to the outboard accumulation of impurities [3, 5], in ICRH-heated plasmas with the resonance layer located at the low magnetic field side (LFS) it is possible to reverse the side of the impurity accumulation from the outboard to the inboard. This effect has been recently recognized as a beneficial factor for controlling the impurity transport since the inboard accumulation of impurities can lead to the reduction of the impurity peaking factor in the core [6–8].

In a recent work [9], the poloidal asymmetry of the impurity ions in ICRH-heated tokamak plasmas has been analyzed. One of the most important parameters governing the impurity

asymmetry strength has been identified to be the minority ion temperature anisotropy, $\alpha_T = T_\perp/T_\parallel$: the ratio of the perpendicular to the parallel temperature of the cyclotron heated minority population. The dependence of α_T on various plasma and ICRH parameters, such as ICRH power, minority and impurity concentrations, bulk plasma density and temperature, has been calculated. In the present paper we extend this work by studying the effects of the ICRH resonance location and plasma shaping on the minority temperature anisotropy.

2. Minority temperature anisotropy

In previous work [9], the poloidal impurity asymmetry strength has been shown to be proportional to the dimensionless parameter $k = \epsilon b_c(\alpha_T - 1)/[b_c + \alpha_T(1 - b_c)]$. Here, $\epsilon = r/R_0$ is the local inverse aspect ratio (r denotes the radial coordinate and R_0 is the plasma major radius), and $b_c = B_c/B_0$, where B_0 and B_c is the magnetic field at the plasma axis and at the minority cyclotron resonance layer, respectively. The parameter b_c, which depends on the location of the minority cyclotron resonance layer in the plasma, is controlled by the choice of B_0 and the radiofrequency (RF) generator frequency, f

$$b_c = \frac{f(\mathrm{MHz})}{15.25\, B_0(\mathrm{T})} \frac{A_\mathrm{m}}{Z_\mathrm{m}},$$

where A_m and Z_m are the atomic mass and the charge number of the resonant minority species. The parameter k also includes the minority temperature anisotropy α_T, which depends on many plasma and ICRH parameters in a complicated way, as was shown by numerical modelling in [9]. It has a maximum close to the resonance location and it increases approximately linearly with the ICRH power unless the heating power is too low. It is generally reduced with the minority concentration since the deposited RF energy per particle is lower. However, it has to be noted that α_T is not simply inversely proportional to the minority ion fraction, as the minority concentration affects the deposition profiles and ICRH power density reached. Minority temperature anisotropy as a function of plasma density scales roughly as $1/n_e^2$, but exhibits oscillations due to the sensitivity of the RF field pattern to multiple reflections and the interference undergone by the RF waves [10–15].

In this work we study the effect of the ICRH resonance location and plasma shaping (ellipticity κ and triangularity δ) on α_T. It is expected that the geometrical factors will affect the wave focussing and the ICRH power density, which determines the minority ion distribution function. The power density values are commonly smaller for the elliptical and D-shaped plasmas since the power absorption is spread over a larger region than in a circular case [16]. The ICRH resonance location is an additional parameter which is expected to affect significantly the impurity asymmetry strength. In Alcator C-Mod experiments, using B_0 scans to modify the location of the hydrogen minority resonance layer, clear 'in-out' asymmetry was observed only for the LFS heating. It is therefore instructive to determine the sensitivity of the reached temperature anisotropy to the ICRH resonance location.

In the general case, the RF field distribution and power deposition profiles in 2D tokamak geometry can only be determined numerically with a full-wave ICRH code. The analysis is further complicated by the fact that by modifying the resonance location one changes not only the minority absorption profile, but the local plasma parameters which determine the energetic minority distribution function (e.g. plasma density and temperature) are also different for different resonance locations. This motivates the use of numerical tools for the analysis of the effect of plasma shaping and cyclotron resonance location on the minority temperature anisotropy.

3. Numerical modelling and results

The temperature anisotropy is computed by the 2D full-wave TORIC code [17, 18] and the Fokker-Planck quasilinear solver SSFPQL [19] and the results are benchmarked to SELFO [20] simulations in the circular cross-section case. SELFO solves the wave field and the distribution function of the resonant ion species self-consistently, including finite-orbit width effects for the high-energy ions and RF-induced transport, but in its current status it cannot handle plasma shaping. TORIC solves Maxwell's equations in an axisymmetric but otherwise arbitrary toroidal magnetic configuration. Maxwellian distribution is assumed for all ion species, including minorities. The flux surface averaged power deposition profiles obtained by TORIC are exported to the quasilinear Fokker-Planck code SSFPQL [19], which evaluates the minority distribution function. SSFPQL provides information on the radial profiles of the high-energy tails generated by ICRH (distribution functions, perpendicular and parallel energies, number of fast ions), and on the collisional exchanges between the various species, but it does not account for toroidal effects (e.g. trapping or finite orbit width). SSFPQL calculates effective perpendicular and parallel temperatures for both the thermal and the tail parts of the distribution and an estimate for the fraction of fast minorities in the tail. Although the absorption and the local temperatures are different in TORIC-SSFPQL and SELFO, the average temperature is comparable, as it has been shown by comparison with self-consistent SELFO simulations presented in [9]. Therefore we expect that the averaged temperature anisotropy obtained by TORIC-SSFPQL gives a reasonable approximation in spite of the simplifying assumptions.

As a reference case we consider hydrogen minority heating in deuterium plasma with the minority concentration $X[\mathrm{H}] = 5\%$ for typical JET-like parameters: $R_0 = 3.0\,\mathrm{m}$, $a = 0.9\,\mathrm{m}$ (plasma minor radius), central electron density $n_{e0} = 3.6\times10^{19}\,\mathrm{m}^{-3}$, central plasma temperature $T_0 = 5.0\,\mathrm{keV}$ (background ions and electrons are assumed to have equal temperatures), the RF generator frequency $f = 41.2\,\mathrm{MHz}$, fast wave toroidal wavenumber $n_{\mathrm{tor}} = 27$, which is dominant for the dipole phasing of the JET A2 ICRH antenna [21,22], $B_0 = 3.0\,\mathrm{T}$, the safety factor at the center and the edge, $q_0 = 1.1$ and $q_1 = 4.5$, respectively. The model density and temperature profiles used in the simulations are $n_e(r) = n_{e0}[1 - 0.5(r/a)^2]$, $T(r) = T_0\,[1 - 0.5(r/a)^2]^{1.5}$. The ICRH power coupled to the plasma is assumed to be $P_{\mathrm{ICRH}} = 3.0\,\mathrm{MW}$. This choice of B_0 and f sets the fundamental hydrogen resonance layer to be located 33 cm to the LFS from the magnetic axis ($R_{\mathrm{H}} = 3.33\,\mathrm{m}$). To study the effect of plasma shaping on α_T for the reference heating scenario the ellipticity has been varied from $\kappa = 1$ to 1.6, and the triangularity from $\delta = 0$ to 0.4. The effect of the ICRH resonance location on α_T has been assessed by studying two additional cases $B_0 = 2.9$ T and $B_0 = 3.1$ T that correspond to $R_{\mathrm{H}} = 3.22\,\mathrm{m}$ and $R_{\mathrm{H}} = 3.44\,\mathrm{m}$, respectively.

For the reference case considered the flux surface averaged profile of the RF power absorbed by minority ions is presented in Fig. 1(a) with the red solid line. The heating maximum is reached at $r/a = 0.29$ and the radial width of the absorption profile (full width at half maximum, FWHM) is $\sim 11.5\,\mathrm{cm}$. Hydrogen minority ions absorb $p_{\mathrm{H}} = 86.6\%$ of the ICRH power, deuterium majority ions – $p_{\mathrm{D}} = 8.5\%$, and the rest of the incident ICRH power is deposited on electrons, $p_{\mathrm{e}} = 4.9\%$. Figure 1 shows the minority power deposition profiles and temperature anisotropy for different values of the ellipticity of the last closed magnetic surface (LCFS), κ_1. We assume the fixed ellipticity, $\kappa_0 = 1.0$ at the magnetic axis. The fraction of the ICRH power, which is absorbed by hydrogen minority ions, is practically unchanged when varying κ_1: $p_{\mathrm{H}} = 87.1\%$ for $\kappa_1 = 1.3$ and $p_{\mathrm{H}} = 87.6\%$ for $\kappa_1 = 1.6$. Figure 2 depicts the power deposition by minority ions in the poloidal cross-section. Clearly, the wave focussing is reduced for an elliptical plasma in comparison with the circular case. For elongated plasmas the power absorption is deposited in a larger volume that results in smaller power density values (Fig. 1(a)). Accordingly, the minority temperature anisotropy decreases for the elongated plasma as Fig. 1(b) illustrates. In the circular case the maximum temperature anisotropy is $\alpha_{\max} = 8.0$, whereas in the elliptic case $\alpha_{\max} = 6.8$ and

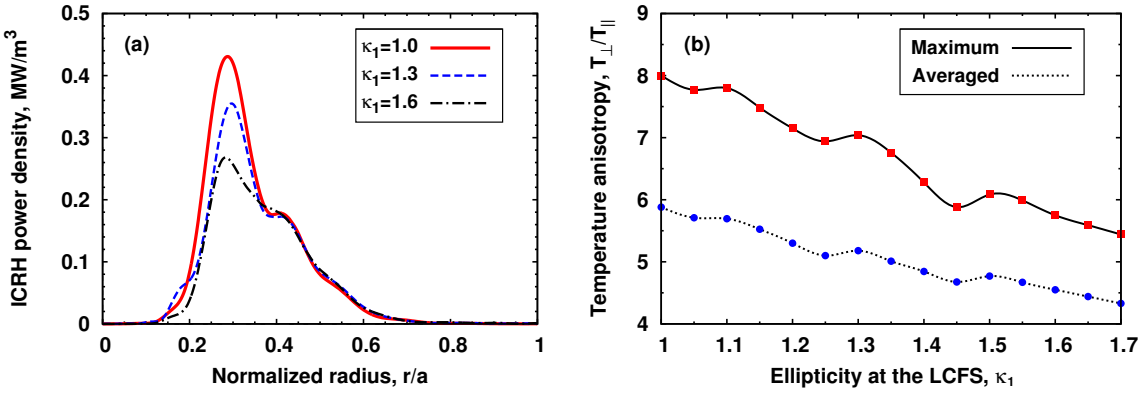

Figure 1. Flux surface averaged absorption profiles (a) and minority temperature anisotropy (b) evaluated by the TORIC-SSFPQL for various values of the ellipticity at the LCFS. The input ICRH power is $P_{\mathrm{ICRH}} = 3.0\,\mathrm{MW}$.

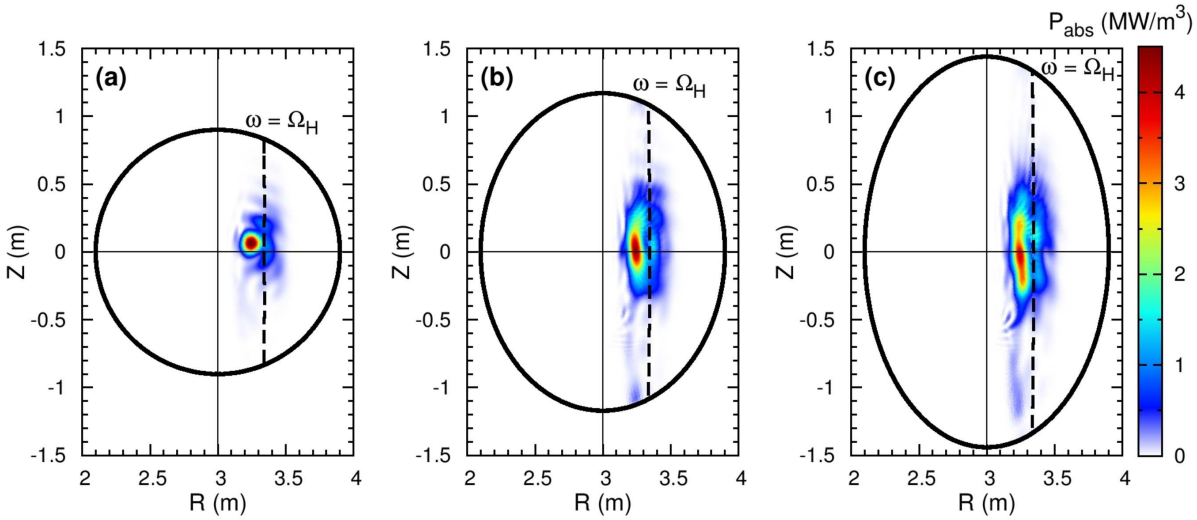

Figure 2. Contour plots of the RF power deposition to hydrogen minority ions in the poloidal cross-section from the TORIC simulations for different values of the edge ellipticity: (a) κ_1=1.0, (b) κ_1=1.3, (c) κ_1=1.6.

$\alpha_{\max} = 5.8$ for $\kappa_1 = 1.3$ and $\kappa_1 = 1.6$, respectively. The same conclusion applies to the averaged temperature anisotropy $\bar{\alpha}$, which is evaluated by averaging the temperature anisotropy over the radial range between FWHM points: $\bar{\alpha} = 5.9$, $\bar{\alpha} = 5.1$, $\bar{\alpha} = 4.6$ for $\kappa_1 = 1$, $\kappa_1 = 1.3$ and $\kappa_1 = 1.6$, respectively. As a result, more ICRH power needs to be coupled to an elongated plasma to achieve the same minority temperature anisotropy than that in a circular case.

For a fixed plasma elongation, the triangularity of the magnetic surfaces has much weaker effect on the power deposition profiles and, consequently, on the minority temperature anisotropy as shown in Fig. 3, which was calculated for $\kappa_1 = 1.6$. Figure 3(b) demonstrates that α_T slightly increases with the triangularity: for $\delta = 0.3$ $\alpha_{\max}$ and $\bar{\alpha}$ reach the values 6.9 and 5.1, respectively. For the heating scenario considered the Shafranov shift is also found to be of marginal importance on the values of the minority temperature anisotropy. Note that the

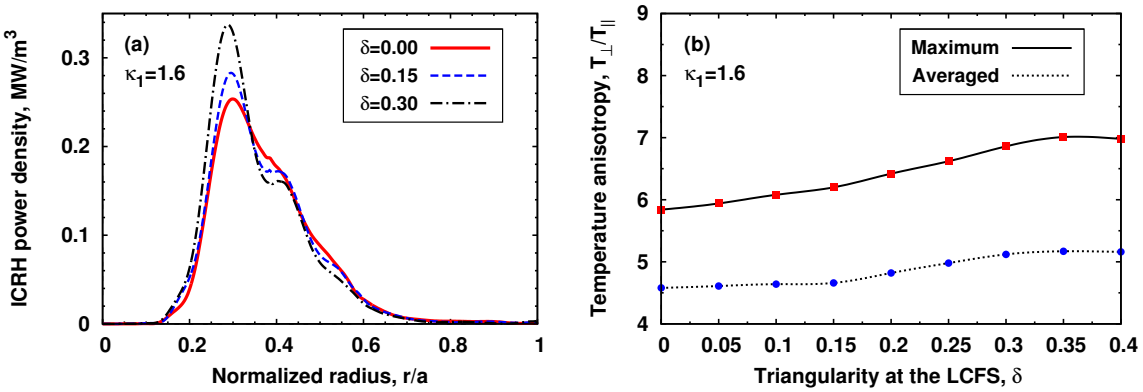

Figure 3. Flux surface averaged absorption profiles (a) and minority temperature anisotropy (b) evaluated by the TORIC-SSFPQL for various values of the plasma triangularity. The LCFS ellipticity is $\kappa_1 = 1.6$.

triangularity of the LCFS has much greater effect on the coupling efficiency [23, 24]. When the LCFS has the same curvature as the ICRH antenna facing the plasma, one commonly gets better coupling of the RF energy from the ICRH antenna to the plasma that results in the improved heating performance.

Figure 4 shows the profiles of the RF power absorbed in the poloidal cross-section (circular case) by hydrogen minority ions for $B_0 = 2.9\,\mathrm{T}$ and $B_0 = 3.1\,\mathrm{T}$. Figures 4(a,c) were calculated with TORIC assuming the Maxwellian background for all plasma species, while Figs. 4(b,d) were calculated with SELFO accounting self-consistently for the change in the minority distribution function. The corresponding radial absorption profiles are depicted in Fig. 5. One should note the difference in the absorption profiles predicted by TORIC and SELFO. While the TORIC profiles are typically peaked, SELFO predicts more radially smoothed absorption. This difference is caused by the simplifying assumption of the Maxwellian distribution for the heated hydrogen minorities underlying the TORIC modelling. Though it is possible to account for the change in the minority distribution function and its effect on the wave propagation and absorption in the TORIC-SSFPQL package [25, 26], the simulations made in the default TORIC mode allows one to get quick qualitative estimates for the temperature anisotropy and its parametric dependences since the averaged power densities and, accordingly, averaged perpendicular energies reached by the heated minorities are comparable for the two different approaches. The fraction of the RF power absorbed by minority ions is also in a fair agreement: for $B_0 = 3.1\,\mathrm{T}$ TORIC predicts $p_\mathrm{H} = 89.3\%$, while SELFO yields $p_\mathrm{H} = 91.6\%$ for the Maxwellian hydrogen distribution and $p_\mathrm{H} = 94.5\%$ in a steady-state.

For the fixed RF generator frequency, by increasing/decreasing the central magnetic field one causes the cyclotron resonance layer and, consequently, the power absorption region to be shifted towards the outer/inner side of the torus (see, Fig. 6(a)). According to TORIC results, for $B_0 = 3.1\,\mathrm{T}$ the heating maximum is observed closer to the edge ($r/a = 0.42$), while for $B_0 = 2.9\,\mathrm{T}$ it is located closer to the magnetic axis ($r/a = 0.15$). The flux surface averaged ICRH power density, which determines the perpendicular minority tail temperature, decreases with increasing B_0 due to the geometrical reasons. Since the RF power is deposited in a smaller volume as r decreases, the absorbed power density increases as the wave absorption takes place closer to the axis. For example, the maximum power density for $B_0 = 2.9\,\mathrm{T}$ is 1.6 times higher than that for $B_0 = 3.0\,\mathrm{T}$. Although the temperature anisotropy scales linearly with the ICRH power density, α_max and $\bar{\alpha}$ are only 1.3 times larger for $B_0 = 2.9\,\mathrm{T}$ than that for the reference

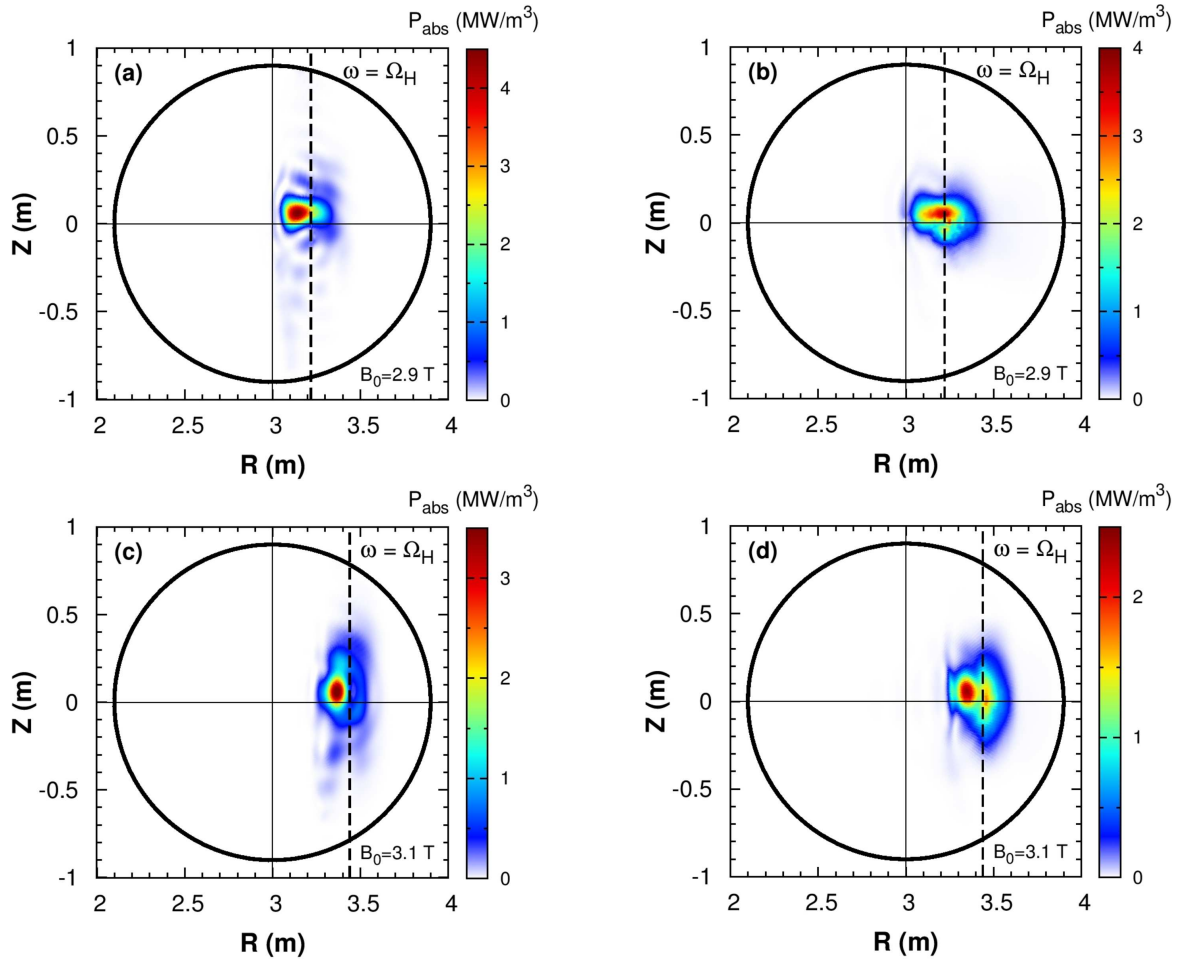

Figure 4. Contour plots of the RF power deposition to hydrogen minority ions in the poloidal cross-section calculated with the TORIC (a,c) and the SELFO (b,d) codes for $B_0 = 2.9\,\mathrm{T}$ and $B_0 = 3.1\,\mathrm{T}$.

case. This is due to the fact that the local plasma density at the absorption region changes when one shifts the ICRH resonance location. Since the temperature anisotropy scales roughly as $\alpha_T \propto 1/n_e^2$, it counteracts the anisotropy increase due to the increase of the local ICRH power density. The decrease of the minority absorption coefficient, p_H in case of the power deposition closer to the center (p_H=83.5% for $B_0 = 2.9\,\mathrm{T}$ and p_H=89.3% for $B_0 = 3.1\,\mathrm{T}$) is caused by the higher plasma temperature within the deposition region that favours the deuterium second harmonic and electron absorption mechanisms. Note, that the higher temperature anisotropy which is predicted for the case of the deposition closer to the axis does not necessarily lead to the higher impurity asymmetry strength since the latter parameter also includes dependence on the inverse aspect ratio and resonance magnetic field (see, Eq. (5) in Ref. [9]).

The non-monotonic dependence of the maximum temperature anisotropy seen in Fig. 1(b) and Fig. 6(b) is likely to be caused by the fact that the wave focussing and RF field pattern are intrinsically sensitive to the actual magnetic field geometry and multiple wave reflections in a plasma. By changing the central magnetic field, one changes the relative location of the absorption region and the high field side fast wave cutoff and thus affects the interference conditions that results in a modulation of the curves. However, it is clearly seen that for

the averaged anisotropy such a modulation is substantially moderated. Thus, accounting for the different waves in the excited antenna spectrum, this effect is unlikely to be observed experimentally.

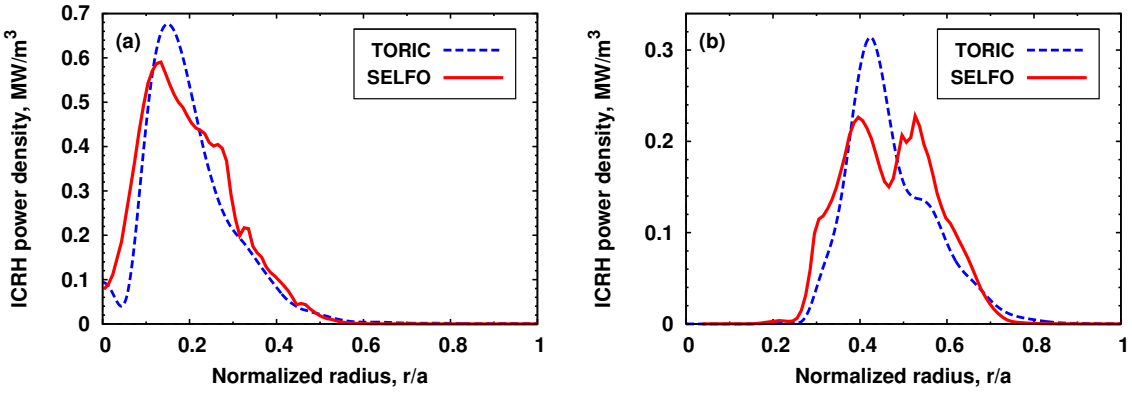

Figure 5. Flux surface averaged deposition profiles to hydrogen minority ions calculated with the TORIC (dashed) and the SELFO codes (solid) for $B_0 = 2.9\,\mathrm{T}$ (a) and $B_0 = 3.1\,\mathrm{T}$ (b).

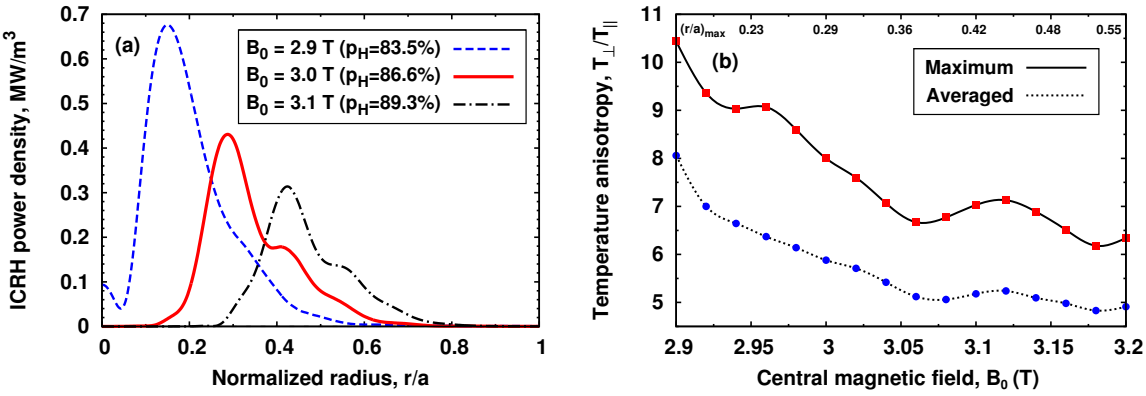

Figure 6. Flux surface averaged absorption profiles (a) and minority temperature anisotropy (b) evaluated by the TORIC-SSFPQL for different central magnetic field B_0.

4. Conclusions

In plasmas heated with the LFS ICRH, the inboard impurity accumulation is often observed. Such an asymmetry in impurity density has been recently considered as a possible mechanism for controlling the impurity transport. The asymmetry arises due to the accumulation of the cyclotron heated minority ions at the outboard side of the magnetic surface leading to the generation of the poloidal electrostatic electric field that pushes impurities to the opposite side. The minority temperature anisotropy has shown to be one of the main factors, which determines the impurity asymmetry strength. The temperature anisotropy depends on most of plasma and heating parameters, and in general case it should be evaluated numerically using the full-wave ICRH and Fokker-Planck codes. The difference in the power deposition profiles predicted by

the TORIC and the SELFO codes is found to be appreciable, but it is not significant for the averaged anisotropy.

By means of the TORIC-SSFPQL modelling we analyzed the effect of plasma shaping and ICRH resonance location on the minority temperature anisotropy in tokamak plasmas. Accounting for the finite ellipticity of the flux surfaces a gradual decrease in the temperature anisotropy is observed which is caused by the wave defocussing and radially broader absorption regions for the elongated plasmas. The temperature anisotropy decrease in case of the resonance layers located closer to the LFS edge is shown. The lower values of the perpendicular minority temperatures are caused by the significant reduction in local surface averaged ICRH power densities due to geometrical reasons.

Acknowledgments

The authors are grateful to Dr. M. Brambilla and Dr. R. Bilato (IPP-Garching) for providing the TORIC-SSFPQL code. Computations for this article have been performed on the HPCFF cluster at the Jülich Supercomputing Center (JSC), Germany. This work was funded by the European Communities under Association Contract between EURATOM and *Vetenskapsrådet*. The views and opinions expressed herein do not necessarily reflect those of the European Commission.

References

[1] Ingesson L C, Chen H, Helander P and Mantsinen M J 2000 *Plasma Phys. Control. Fusion* **42** 161.
[2] Marr K D, Lipschultz B, Catto P J, McDermott R M, Reinke M L and Simakov A N 2010 *Plasma Phys. Control. Fusion* **52** 055010.
[3] Reinke M L *et al.* 2012 *Plasma Phys. Control. Fusion* **54** 045004.
[4] Choe W, Chang C S and Ono M 1995 *Phys. Plasmas* **2** 2044.
[5] Alper B, Edwards A W, Giannella R, Gill R D, Ingesson C, Romanelli M, Wesson J and Zastrow K-D 1996 *Proc. 23rd EPS Conf. on Plasma Phys. and Contr. Fusion* (Kiev, Ukraine) ECA **20C** p. 163–166.
[6] Fülöp T and Moradi S 2011 *Phys. Plasmas* **18** 030703.
[7] Moradi S, Fülöp T, Mollén A and Pusztai I 2011 *Plasma Phys. Control. Fusion* **53** 115008.
[8] Mollén A, Pusztai I, Fülöp T, Kazakov Ye O and Moradi S 2012 *Phys. Plasmas* **19** 052307.
[9] Kazakov Ye O, Pusztai I, Fülöp T and Johnson T 2012 *Plasma Phys. Control. Fusion* **54** 105010.
[10] Majeski R, Phillips C K and Wilson J R 1994 *Phys. Rev. Lett.* **73** 2204.
[11] Fuchs V, Ram A K, Schultz S D, Bers A and Lashmore-Davies C N 1995 *Phys. Plasmas* **2** 1637.
[12] Van Eester D *et al.* and JET EFDA contributors 2009 *Plasma Phys. Control. Fusion* **51** 044007.
[13] Kazakov Ye O, Pavlenko I V, Van Eester D, Weyssow B and Girka I O 2010 *Plasma Phys. Control. Fusion* **52** 115006.
[14] Van Eester D *et al.* and JET EFDA Contributors 2012 *Plasma Phys. Control. Fusion* **54** 074009.
[15] Kazakov Ye O, Kiptily V G, Sharapov S E, Van Eester D and JET EFDA Contributors 2012 *Nucl. Fusion* **52** 094012.
[16] Van Eester D, Bhatnagar V P and Koch R 1985 *Plasma Phys. Control. Fusion* **27** 1015.
[17] Brambilla M 1999 *Plasma Phys. Control. Fusion* **41** 1.
[18] Wright J C, Bonoli P T, Brambilla M, Meo F, D'Azevedo E, Batchelor D B, Jaeger E F, Berry L A, Phillips C K and Pletzer A 2004 *Phys. Plasmas* **11** 2473.
[19] Brambilla M 1994 *Nucl. Fusion* **34** 1121.
[20] Hedin J, Hellsten T, Eriksson L-G and Johnson T 2002 *Nucl. Fusion* **42** 527.
[21] Mayoral M-L *et al.* and JET EFDA contributors 2006 *Nucl. Fusion* **46** S550.
[22] Noterdaeme J-M, Eriksson L-G, Mantsinen M, Mayoral M-L, Van Eester D, Mailloux J, Gormezano C and Jones T T C 2008 *Fusion Sci. Technol.* **53** 1103.
[23] Bilato R, Mayoral M-L, Rimini F, Brambilla M, Hartmann D A, Korotkov A, Lamalle P U, Monakhov I, Noterdaeme J-M, Sartori amd JET EFDA contributors 2004 *Proc. 31th EPS Conf. on Plasma Phys.* (London, UK) ECA **28G** P-5.164.
[24] Bobkov Vl V, Bilato R, Braun F, Dux R, Noterdaeme J-M, the ICRF team and the ASDEX Upgrade team 2006 *Nucl. Fusion* **46** S469.
[25] Brambilla M and Bilato R 2009 *Nucl. Fusion* **49** 085004.
[26] Bilato R, Brambilla M, Maj O, Horton L D, Maggi C F and Stober J 2011 *Nucl. Fusion* **51** 103034.